Int J Biochem Mol Biol 2012;3(1):86-94
www.ijbmb.org /ISSN:2152-4114/IJBMB1202001

Original Article

Structural basis of heparin binding to camel peptidoglycan recognition protein-S

Pradeep Sharma, Divya Dube, Mau Sinha, Sharmistha Dey, Punit Kaur, Sujata Sharma, Tej P. Singh

Department of Biophysics, All India Institute of Medical Sciences, New Delhi, India

Received February 8, 2012; accepted March 14, 2012; Epub March 20, 2012; Published March 30, 2012

Abstract: Short peptidoglycan recognition protein (PGRP-S) is a member of the innate immunity system in mammals. PGRP-S from Camelus dromedarius (CPGRP-S) is found to be highly potent against bacterial infections. It is capable of binding to a wide range of pathogen-associated molecular patterns (PAMPs) including lipopolysaccharide (LPS), lipoteichoic acid (LTA) and peptidoglycan (PGN). The heparin-like polysaccharides have also been observed in some bacteria such as the capsule of K5 Escherichia coli thus making them relevant for determining the nature of their interactions with CPGRP-S. The binding studies of CPGRP-S with heparin disaccharide in solution using surface plasmon resonance gave a value 3.3×10^{-7} M for the dissociation constant (Kd). The structure of the heparin bound CPGRP-S determined at 2.8Å resolution revealed the presence of a bound heparin molecule in the binding pocket of CPGRP-S. It was found anchored tightly to the protein with the help of several ionic and hydrogen bonded interactions. Three sulphate groups of heparin S1, S2 and S3 have been found to interact with residues, Arg-31, Lys-90, Thr-97, Asn-99 Asn-140, Gln-150 and Arg-170 of CPGRP-S. The binding site includes two subsites, S-I and S-II with cleft-like structures. Heparin disaccharide is bound in subsite S-I. Previously determined structures of the complexes of CPGRP-S with LPS, LTA and PGN also showed that their glycan moieties were also held in subsite S-I indicating that heparin disaccharide also represents an important element for the recognition by CPGRP-S.

Keywords: PGRP-S, PAMPs, heparin, crystal structure, LPS, LTA, PGN

Introduction

The protein molecules of mammalian innate immune system [1] include four peptidoglycan recognition proteins (PGRPs), (i) long-PGRP (PGRP-L; M.W. up to 90 kDa) (ii&iii) intermediate-PGRPs (PGRP-Iα and PGRP-Iβ; M.W. 40-45 kDa) and (iv) short PGRP (PGRP-S; M.W. 20-25 kDa) [2]. First three PGRPs have a common C-terminal domain of approximately 165-200 amino acid residues which is known as PGRP domain and is similar to PGRP-S in size, scaffolding and action [3]. Although PGRP-S is expressed in various tissues, its presence in granules of polymorphonuclear leukocytes indicates that it has a role as an antibacterial agent [4]. It has been shown that this protein is also expressed in the lactating mammary glands of mammals [5]. However, so far it has been detected only in the milk of *Camelus dromedarius* [5]. The average concentration of this protein in the camel milk is found to be of the order of 12 mg/100 ml [5]. So far, crystal structures of PGRP-S from only two species, camel (CPGRP-S) [6] and human (HPGRP-S) [7] have been determined. The reported structure of HPGRP-S is that of a truncated polypeptide chain consisting of residues from 9 to 175. It was shown to adopt a monomeric structure, although it is mentioned in literature that it forms a covalently -linked dimer because cysteine at position 8 is assumed to be involved in a disulfide bridge with Cys8 of another HPGRP-S molecule [8]. However, this fact is not yet fully resolved because so far clear experimental evidence is not available about the quaternary state of HPGRP-S. The C-terminal domains of HPGRP-Iα (residues, 177 to 341) and HPGRP-Iβ (residues, 210 to 373) are similar to HPGRP-S [8]. The structure determination of CPGRP-S has shown clearly that the protein molecules form linear polymers repeating two contact surfaces alternatively. The structure and binding studies with lipopolysaccharide (LPS; lipid A), lipoteichoic

acid (LTA; one unit of LTA polymer) [9], peptidoglycan (PGN; acetylmuramyl-alanyl-isoglutamine) [10] have shown that all these ligands bind at one of these two repeating contact sites. Unlike other PGRPs which tend to differentiate between Gram-negative and Gram-positive bacteria and bind selectively to one of them [11], CPGRP-S binds to both types of bacterial surfaces with nearly similar affinities [9, 10]. In view of this, it is pertinent to examine the full range of versatility of the binding by CPGRP-S to a variety of bacterial cell surface molecules so that the potential of its clinical applications could be realized. Therefore, we have carried out binding studies of CPGRP-S with heparin disaccharide and determined the crystal structure of CPGRP-S complexed with heparin disaccharide. The structure determination showed that heparin disaccharide binds to CPGRP-S tightly and forms a number of contacts with protein atoms including ionic, hydrogen bonded and van der Waals interactions. It was noteworthy that the binding region occupied by heparin in CPGRP-S is the same as reported for the glycan moieties of LPS [9], LTA [9] and PGN [10]. However, it may be mentioned here that the structures of the complexes of human C-terminal domain of PGRP-Iα with muramyl tripeptide (MTP) [12] and human C-terminal domain of PGRP-Iβ with muramyl pentapeptide (MPP) [13] have been reported.

Materials and methods

Purification of protein

Fresh mammary gland secretions of camel were obtained from the National Research Center on Camels (NRCC), Bikaner, India. The protein was purified to homogeneity from fresh camel milk samples using a two step column chromatography as described earlier [6]. The purity of protein was checked on sodium dodecyl sulphate-polyacrylamide gel electrophoresis (SDS-PAGE) and matrix assisted laser desorption /ionization-time of flight (MALDI-TOF) that showed a single band on SDS-PAGE and one peak in MALDI-TOF. The amino acid sequence [5] of CPGRP-S showed that it lacks potential glycosylation sites with Asn-X-Ser/Thr sequence motifs.

Surface plasmon resonance spectroscopy

The direct binding experiments were carried out using a BIAcore 2000 instrument (BIAcore, Uppsala, Sweden) as described previously [6]. The methodology used is based on surface plasmon resonance (SPR). CPGRP-S was covalently coupled to a CM5 Sensor Chip (BIAcore) following the manufacturer's instructions. The control flow-cells consisted of immobilized bovine serum albumin (BSA). Heparin disaccharide obtained from Sigma-Aldrich (St Louis, MO, USA) was dissolved in PBS and injected at a flow rate of 10 µl/min at 25°C using the multichannel mode. The regeneration of the sensor surface was achieved by short pulses of 0.1 M NaOH or/and repeated washes with buffer. The data analysis was carried out with BIAcore 3.0 evaluation software provided by the manufacturer.

Crystallization

The purified samples of protein were dissolved in the buffer containing 50mM Tris-HCl, pH 8.0 to a final concentration of 15 mg/ml. 10 µl of protein solution was mixed with equal volume of the reservoir solution containing 10% Polyethylene glycol-3350 (PEG-3350) and 0.2 M Sodium potassium tartrate. The 10 µl drops of protein solution were set up in the hanging drop vapor diffusion setup against the above reservoir solution. Crystals appeared after about a week. The freshly grown crystals of CPGRP-S were soaked in the reservoir solution containing heparin disaccharide at a concentration of 30 mg/ml.

X-ray intensity data collection and processing

The soaked crystals of CPGRP-S were stabilized in the reservoir solution to which 30% glycerol was added for the data collection at low temperature. A single crystal was mounted in a nylon loop and flash - frozen in a stream of nitrogen gas at 100 K. The data were collected using the DBT-sponsored beamline BM-14 at ESRF, Grenoble, France with a wavelength, λ = 0.98 Å using a 165 mm MAR CCD detector (MAResearch, Norderstedt, Germany). The data were processed with DENZO and SCALEPACK from HKL package [14]. The final data set was complete to 96.2% to 2.8 Å resolution. The crystals belong to orthorhombic space group I222 with unit cell dimensions of a = 88.4 Å, b = 101.7 Å, c = 162.8 Å. The presence of four molecules per asymmetric unit gave a crystal volume (Vm) of 2.41 $Å^3Da^{-1}$ per protein mass corresponding to a solvent content of 48.8% by volume. The results of data collection and proc-

Table 1. Data Collection and refinement statistics for the structure of the complexe of camel peptidoglycan recognition protein (CPGRP-S) with Heparin (HEP).

	PGRP-S + HEP
PDB ID	3OGX
Space group	I222
Unit cell dimensions	
a (Å)	88.4
b (Å)	101.7
c (Å)	162.8
Number of molecules in the asymmetric unit	4
Vm (Å^3/Da)	2.41
Solvent Content (%)	48.8
Resolution range (Å)	47.9-2.80
Total number of measured reflections	248232
Number of unique reflections	33492
#Rsym (%)	8.9 (28.9)
I/σ(I)	17.0 (3.5)
Overall completeness of data (%)	96.2 (84.2)
*R_{cryst} (%)	20.5
R_{free} (%)	23.4
Protein atoms	5348
Water oxygen atoms	303
Atoms of heparin disaccharide	35
Atoms of tartrate	10
Atoms of glycerol	6
R.m.s.d in bond lengths (Å)	0.01
R.m.s.d in bond angles (°)	2.0
R.m.s.d in torsion angles (°)	24.8
Mean B-factor for main chain atoms (Å^2)	36.0
Mean B-factor for side chain atoms (Å^2)	39.2
Mean B-factor for all atoms(Å^2)	37.8
Ramachandran's φ, ψ map	
Residues in the most favoured regions (%)	90.8
Residues in the additionally allowed regions (%)	9.2

The values in parentheses correspond to the values in the highest resolution shell. #$R_{sym} = \Sigma_{hkl}\Sigma_i |I_i(hkl) - \langle I(hkl)\rangle| / \Sigma_{hkl}\Sigma_i I_i(hkl)$; *$R_{cryst} = \Sigma_{hkl} |F_o(hkl) - F_c(hkl)| / \Sigma_{hkl}|F_o(hkl)|$ where F_o and F_c are observed and calculated structure factors respectively.

essing are given in **Table 1**.

Structure determination and refinement

Crystal structure of the complex was determined using molecular replacement method with program MOLREP [15]. The coordinates of a monomer from the structure of native CPGRP-S (PDB ID: 3C2X) were used as a model for the structure determination. It yielded a clear solution. The refinement was carried out with program CNS [16]. At each refinement step $|2F_o - F_c|$ and $|F_o - F_c|$ maps were calculated for manual model building using the program O [17] on Silicon Graphics O2 workstation. A subset comprising 2% of the reflections was not used in the refinement to allow for calculations of free R-factor. Further cycles of refinement reduced the crystallographic R-factor to 0.281 (free R-factor to 0.311). At this stage a non-protein electron density at 2.0σ cut off in the $|F_o - F_c|$ map was observed into which heparin disaccharide was modelled (**Figure 1A**). At the same time (2Fo-Fc) map was also calculated for the region where heparin disaccharide binding occurred to show relative density at 1.2σ cut off (blue) for heparin disaccharide and surrounding residues. A density map (2Fo-Fc) at high cut off at 2.5σ (red) was also drawn. It showed comparable electron densities for both protein residues and heparin disaccharide (**Figure 1B**). At this stage, the positions of water oxygen atoms were also determined when observed as spherical peaks at a level of at least 3.0σ in $|F_o - F_c|$ maps, provided they formed suitable hydrogen bonds with protein partners in the model. The water molecules that failed to appear at 2.0σ in the subsequent $|2F_o - F_c|$ maps following further rounds of re-

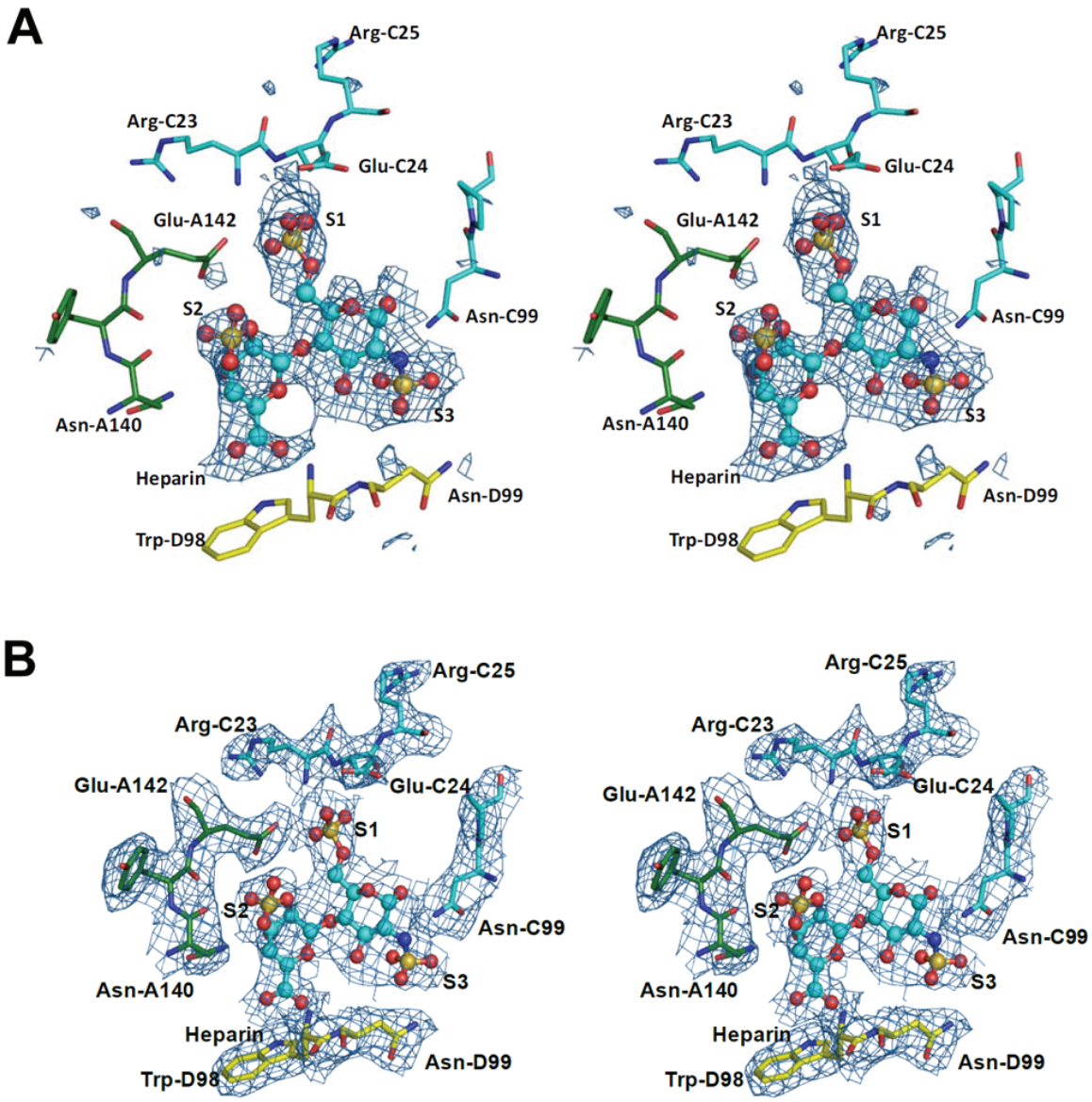

Figure 1. (A) Stereoview of the initial (Fo-Fc) electron density map at 2σ cut off. The neighbouring residues from molecules A, B, C and D are also indicated. (B) Stereoview of the omit map calculated during final stages of the refinement of by omitting heparin disaccharide and surrounding residues of the binding subsite S-I at 2.5σ cut off.

finement were removed from the model. Towards the end of refinement, additional sites with non-protein electron densities at 2.5σ cut-off in the $|F_o - F_c|$ map were also observed into which one tartrate molecule and one glycerol molecule were fitted and added into the model and refined. The refinement using a bulk solvent model was included in the final stages that resulted in considerable improvement in the R-factor for data in the low-resolution shell. The final values of R_{cryst} and R_{free} factors were 20.5% and 23.4% respectively. The quality of the model was assessed using PROCHECK [18]. The coordinates for the final model have been deposited at Rutgers University Protein Data Bank with accession code 3OGX.

Results

Surface plasmon resonance spectroscopic analysis

The evaluation of binding affinity of heparin disaccharide towards CPGRP-S was carried out

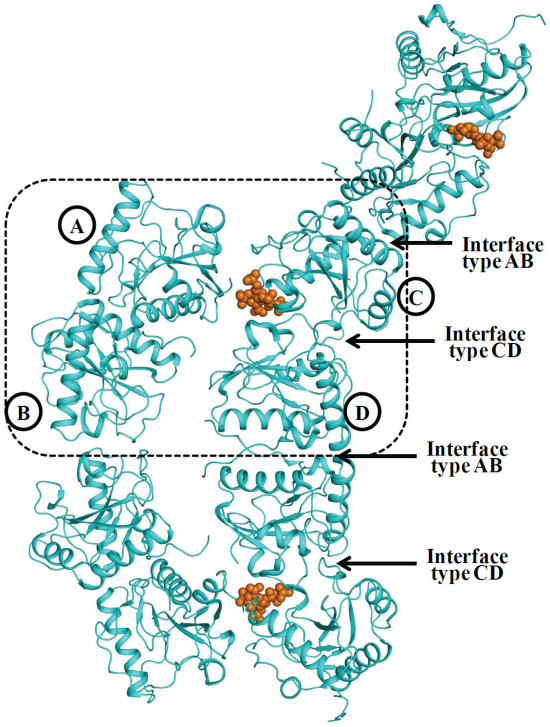

Figure 2. (A) SPR sensograms showing the association and dissociation curves for the binding of heparin disaccharide. CPGRP-S was immobilized on CM-5 chip and three concentrations (1.4 mM, 2.5 mM and 5.0 mM) of analyte heparin disaccharide were used in the mobile phase. The corresponding curves are indicated by a, b and c respectively. (B) The fitted curves are shown by dotted lines.

using the real time surface plasmon resonance (SPR) spectroscopy. The SPR sensograms illustrating the nature of association and dissociation for heparin disaccharide are given in **Figure 2A**. The curve-fitting process was also carried out which showed a good agreement on fitting the data (**Figure 2B**). The overall fitting of the observed data to the 1:1 association model obtained with BIA-evaluation 3.0 software package gave the value of 3.3×10^{-7} M for the dissociation constant (Kd) for the complex of CPGRP-S with heparin disaccharide.

Quality of model

The final model consists of 5348 protein atoms from four crystallographically independent protein molecules in the asymmetric unit, a tightly bound heparin disaccharide, a tartrate molecule bound at the C-D interface and one glycerol molecule located at the surface (**Figure 3**). The positions of 303 water oxygen atoms were also determined using difference Fourier maps (Fo-Fc). The final crystallographic R-factor is 20.5% (R_{free} = 23.4%). A Ramachandran plot [19] for the whole protein molecule shows 90.8% of residues in the most favoured regions as calculated using PROCHECK [18]. The summary of refinement statistics is given in **Table 1**.

Overall structure

The structure determination of CPGRP-S re-

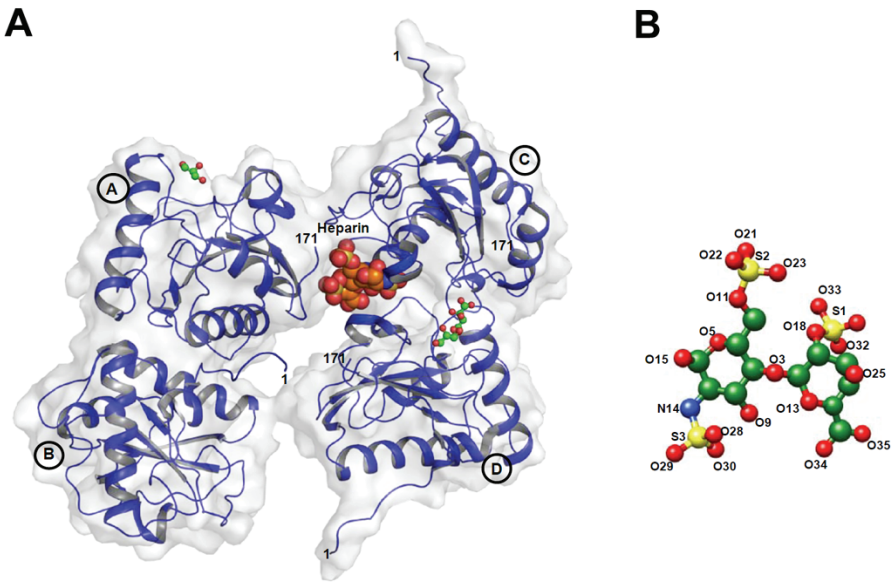

Figure 3. (A) Ribbon diagram for four crystallographically independent molecules A, B, C and D representing A-B and C-D units of neighbouring CPGRP-S linear polymers. Heparin disaccharide is bound to protein molecule C at subsite SI. The ligand binding cleft in the tetramer is indicated by segments which are highlighted in red. The molecules of tartrate and glycerol are also shown (in ball and stick representation). (B) Heparin molecule with atom numbering is shown.

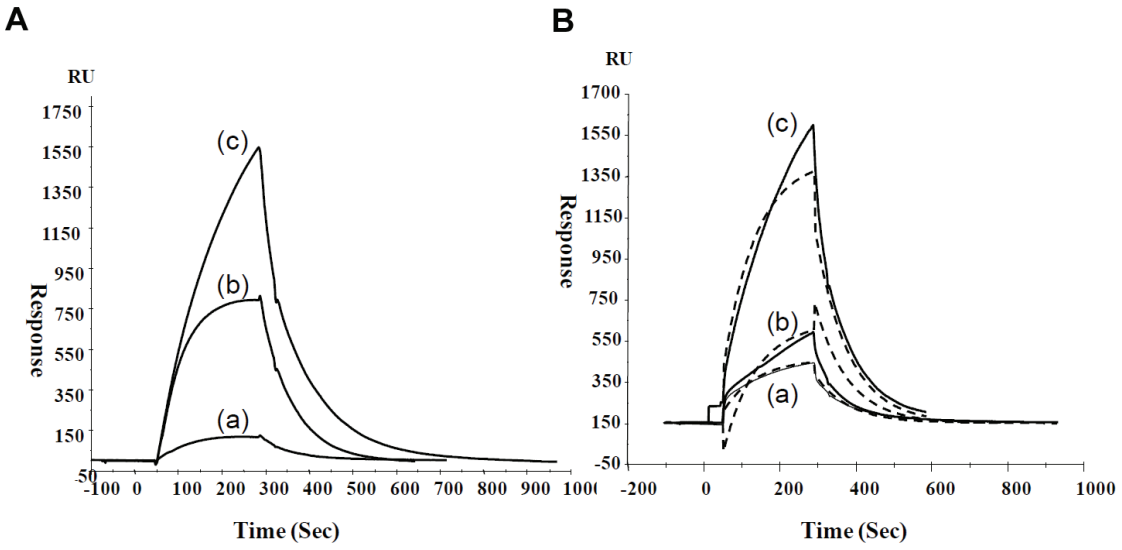

Figure 4. The columns of linear polymers of CPGRP-S with alternating contacts A-B and C-D. Heparin disaccharide molecules are bound to molecule C at C-D contact site.

vealed that the asymmetric unit of the unit cell contains four crystallographically independent protein molecules which are designated as molecules A, B, C and D. The superimpositions of their C^{α}-traces on each other showed rms shifts in the range of 0.3Å to 0.6Å indicating that their polypeptide chains folded in an identical manner. As seen from **Figure 4**, molecules A, B, C and D represent A-B and C-D units of two neighbouring linear polymers of CPGRP-S stacked parallelly in the crystals. These polymers are stabilized by alternating A-B and C-D contacts. The buried interface area as calculated using PISA [18] for A-B contact was found to be 858 $Å^2$ while it was 818 $Å^2$ for the C-D interface. The calculation shows a buried area of approximately 360 $Å^2$ between A and C while the value for B-D interface is 80 $Å^2$. It indicates that the neighbouring linear columns of CPGRP-S molecules with alternating A-B and C-D contacts are connected through A-C contacts. However, when a four molecule unit is considered with A, B, C and D it gave an interface area of 1787$Å^2$ while those in any other symmetry combinations produced smaller buried interface areas of 1043$Å^2$ and 719$Å^2$ respectively. This showed that four crystallographically independent molecules A, B, C and D formed a more stable representation of four subunits.

Interactions between CPGRP-S and heparin disaccharide

Heparin disaccharide is a negatively charged molecule with two glycan residues. The position of heparin disaccharide coincides with the positions of glycan moieties of other PAMPs as observed in the structures of the complexes of CPGRP-S with LPS [9], LTA [9] and PGN [10]. Heparin disaccharide interacts extensively with protein atoms (**Table 2**). There are atleast 19 ionic or hydrogen bonded interactions and approximately 100 van der Waals contacts between CPGRP-S and heparin disaccharide. The sulphate group S1 interacts with Arg-170 (Arg-170 NH1••••••O3 = 3.1 Å) while sulphate moiety S2 is in contact with Lys-90 (Lys-90Nη••••••O22 = 3.3 Å). The third sulphate group S3 forms three hydrogen bonds with Gly-95N••••••O29 = 2.9Å, Asn-99$N^{\delta 2}$••••••O29 = 3.3 Å and Gln-150$O^{\varepsilon 2}$••••••O30 = 3.1 Å (**Figure 5**). The most frequently interacting residues with glycan moieties at the subsite I include Asn-140 and Arg-170 from molecule A, Trp-66, Arg-85, Lys-90, Gly-95 and Asn-99 from molecule C and Thr-97, Val-149 and Glu-150 from molecule D.

Discussion

The crystal structure determination of CPGRP-S had revealed the presence of four crystallographically independent molecules A, B, C and D in the asymmetric unit [6]. The visual inspection of these four subunits indicated that they formed two dimers, A-B and C-D. However, a further analysis of the model using PISA [20] suggested that it formed linear polymers with C-

Table 2. Hydrogen bonded and ionic interactions between CPGRP-S and heparin disaccharide. The letters before residue numbers indicate molecules A, B, C and D of CPGRP-S.

Protein/Water	Heparin/Water	Distance (Å)
Asn - A140 O	O31	2.7
Glu - A142 OE2	O31	3.2
Arg - A170 NE	O33	3.2
Arg - A170 NH1	O33	3.1
Asn - C99 ND2	N14	2.9
Asn - C99 ND2	O15	2.7
Glu - C24 OE1	O21	2.8
Glu - C142 OE1	O21	3.4
Glu - C24 OE1	O22	2.8
Lys - C90 NZ	O22	3.3
Glu - C142 OE1	O23	2.5
Asn - C140 ND2	O25	3.3
Gly - C65 O	O25	3.3
Gly - C95 N	O29	2.9
Asn - C99 ND2	O29	3.3
Trp - C66 NE1	O34	3.1
Thr - D97 OG1	O32	2.6
Gln - D150 NE1	O30	3.1
Val - D149 O	O34	3.3

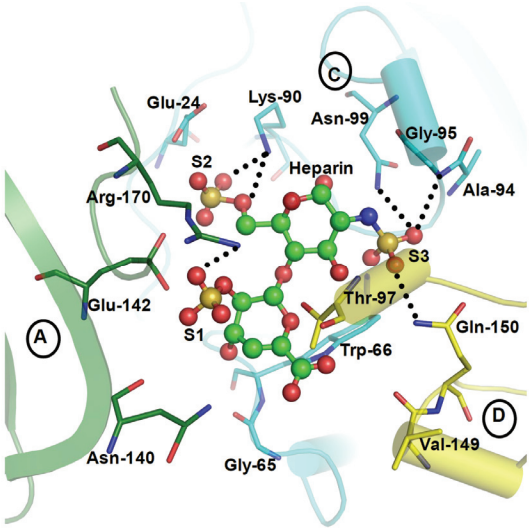

Figure 5. The interactions involving protein atoms (CPGRP-S) with sulphate moieties of heparin disaccharide and protein residues. The sulphate moieties S1 (PDB name: S26) forms an ionic interaction with Arg-A170, S2 (PDB name: S16) forms a salt bridge with Lys-C90 while S3 (PDB name: S20) forms three hydrogen bonds with Ala-C94, Asn-C99 and Glu-D150.

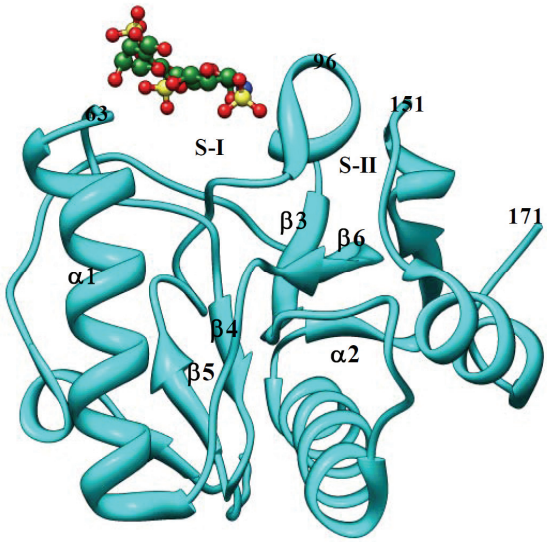

Figure 6. Showing two pockets SI and SII on the ligand binding site of CPGRP-S. Heparin disaccharide binds at subsite I.

D and A-B contacts repeating alternatively (**Figure 4**) as the buried interface areas at two interfaces were comparable. As shown by **Figure 3**, heparin disaccharide bound these columns at the sites of C-D contacts. An examination of intermolecular interactions between protein and heparin disaccharide showed that heparin disaccharide formed atleast 19 hydrogen bonds and nearly 100 van der Waals contacts indicating the formation of a very stable complex of CPGRP-S with heparin disaccharide. In the scheme as shown in **Figure 3,** heparin disaccharide binds primarily to molecule C. In the crystals, it was observed that it also formed a few additional interactions with molecules A and D. As seen from **Figure 5**, the sulphate groups are anchored in the pockets containing residues, Lys-90, Asn-99, Gln-150 and Arg-170. An examination of the ligand binding surface shows two cavity-like subsites separated by a loop His93 – Pro100 in the protein molecule which are indicated as subsites, S-I and S-II (**Figure 6**). Heparin occupies subsite S-I and fills it completely. Subsite S-II in the structure is slightly hindered by a loop from molecule D at the C-D interface of the protein polymer (**Figure 4**). As reported earlier the glycan moieties of other PAMPs, LPS

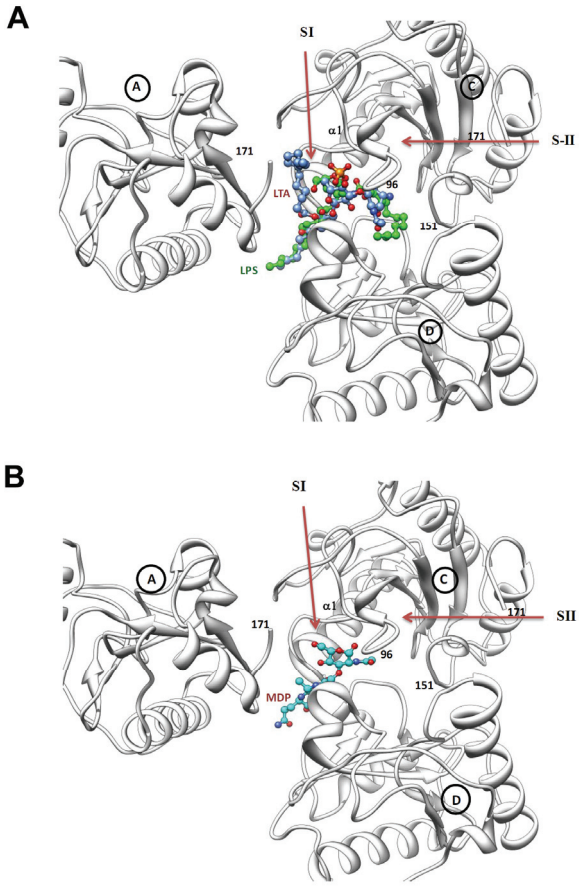

Figure 7. (A) The bindings of LPS (PDB: 3RT4) and LTA (PDB: 304K) to CPGRP-S. The glycan moieties are fitted in the glycan binding pocket while their hydrocarbon chains are adjusted along the molecular surface. (B) The binding of PGN (PDB: 3NW3) to CPGRP-S. The glycan moiety is fixed at glycan binding pocket. The peptide chain is adjusted along the surface of the protein molecule.

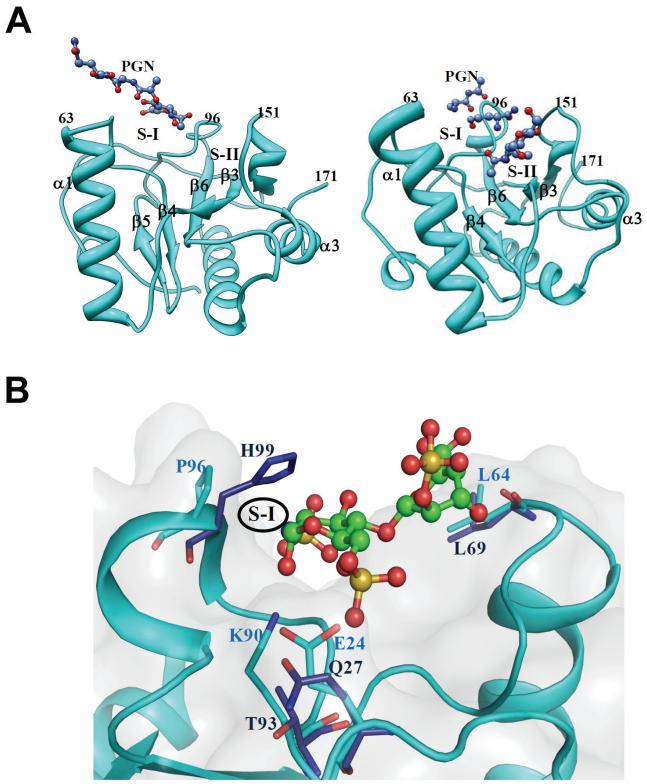

Figure 8. (A) Muramyl dipeptide bound to HPGRP-IαC with peptide moiety at subsite, S-I and glycan moiety at subsite, S-II. (B) Superimposition of subsite S-I from CPGRP-S and HPGRP-S showing an obstruction by His99 in HPGRP-S. The corresponding residue in CPGRP-S is Pro-96. Furthermore, the presence of Glu-24 and Lys-90 in the binding site in CPGRP-S are helpful in the recognition of PAMPs. The corresponding residues in HPGRP-S are Gln-27 and Thr-93.

[8], LTA [8] and PGN [9] were also held at the same subsite S-I. As the glycan moieties get fixed in the glycan binding pocket S-I, the hydrocarbon attachments such as those in LPS and LTA (**Figure 7A**) and peptide chain such as in PGN (**Figure 7B**) are appropriately adjusted on the protein surface. In a contrast, in the complexes of HPGRP-IαC [12] and HPGRP-IβC [13] with MTP and MPP, the glycan moieties were observed at a relatively less specific subsite, S-II due to constraints at subsite, S-I (**Figure 8A**) while peptide moieties were held at subsite, S-I indicating that the peptide moieties formed a more specific component of PGN for the recognition by HPGRP (**Figure 8B**). Since the cross-linking peptides of PGN in Gram-negative bacteria and Gram-positive bacteria contained meso -diaminopimelic acid type (Dap-type) and L-lysine type (Lys-type) respectively, the peptide based recognition of such ligands would require different specificities in PGRPs. In this regard CPGRP-S is different because the initial element of recognition is the glycan moiety of PAMPs. The preference for glycan moiety may partly be due to a unique state of quaternary structure of CPGRP-S where protein molecules form A-B and C-D contacts. As the binding of heparin and other glycan moiety containing ligands occur at the C-D contacts, the ligand binding site in molecule C is further supported by its association with molecule D.

Acknowledgments

This work was supported by the grants from the Departments of Science and Technology (DST) and Department of Biotechnology (DBT), Ministry of Science and Technology, Government of India, New Delhi. MS thanks the Council of Scientific and Industrial Research (CSIR), New Delhi for financial support. PS gratefully acknowledges the DST-INSPIRE Faculty award. TPS thanks DBT for the grant of Distinguished Biotechnology Research Professorship.

Address correspondence to: Dr. Singh TP, Department of Biophysics, All India Institute of Medical Sciences, Ansari Nagar, New Delhi – 110 029, India Tel: +91-11-2658-8931; Fax: +91-11-2658-8663; E-mail: tpsingh.aiims@gmail.com

References

[1] Medzhitov R, Janeway C Jr. Innate immunity. N Engl J Med 2000; 343: 338-344.
[2] Dziarski R, Gupta D. The peptidoglycan recognition proteins (PGRPs). Genome Biol 2006; 7: 232.
[3] Kang D, Liu G, Lundstrom A, Gelius E and Steiner H. A peptidoglycan recognition protein in innate immunity conserved from insects to humans. Proc Natl Acad Sci USA 1998; 95: 10078-10082.
[4] Dziarski R, Platt KA, Gelius E, Steiner H and Gupta D. Defect in neutrophil killing and increased susceptibility to infection with nonpathogenic gram-positive bacteria in peptidoglycan recognition protein-S (PGRP-S)-deficient mice. Blood 2003; 102: 689-697.
[5] Kappeler SR, Heuberger C, Farah Z and Puhan Z. Expression of the peptidoglycan recognition protein, PGRP, in the lactating mammary gland. J Dairy Sci 2004; 87: 2660-2668.
[6] Sharma P, Singh N, Sinha M, Sharma S, Perbandt M, Betzel C, Kaur P, Srinivasan A and Singh TP. Crystal structure of the peptidoglycan recognition protein at 1.8 Å resolution reveals dual strategy to combat infection through two independent functional homodimers. J Mol Biol 2008; 378: 923-932.
[7] Guan R, Wang Q, Sundberg EJ and Mariuzza RA. Crystal structure of human peptidoglycan recognition protein S (PGRP-S) at 1.70 Å resolution. J Mol Biol 2005; 347: 683-691.
[8] Lu X, Wang M, Qi J, Wang H, Li X, Gupta D and Dziarski R. Peptidoglycan recognition proteins are a new class of human bactericidal proteins. J Biol Chem 2006; 281: 5895-5907.
[9] Sharma P, Dube D, Singh A, Mishra B, Singh N, Sinha M, Dey S, Kaur P, Mitra DK, Sharma S and Singh TP. Structural basis of recognition of pathogen-associated molecular patterns and inhibition of proinflammatory cytokines by camel peptidoglycan recognition protein. J Biol Chem 2011; 286: 16208-16217.
[10] Sharma P, Dube D, Sinha M, Mishra B, Dey S, Mal G, Pathak KM, Kaur P, Sharma S and Singh TP. Multiligand Specificity of Pathogen-associated Molecular Pattern-binding Site in Peptidoglycan Recognition Protein. J Biol Chem 2011; 286: 31723-31730.
[11] Liu C, Gelius E, Liu G, Steiner H, Dziarski R. Mammalian peptidoglycan recognition protein binds peptidoglycan with high affinity, is expressed in neutrophils, and inhibits bacterial growth. J Biol Chem 2000; 275: 24490-24499.
[12] Cho S, Wang Q, Swaminathan CP, Hesek D, Lee M, Boons GJ, Mobashery S and Mariuzza RA. Structural insights into the bactericidal mechanism of human peptidoglycan recognition proteins. Proc Natl Acad Sci USA 2007; 104: 8761-8766.
[13] Guan R, Roychowdhury A, Ember B, Kumar S, Boons GJ, Mariuzza RA. Structural basis for peptidoglycan binding by peptidoglycan recognition proteins. Proc Natl Acad Sci USA 2004; 101: 17168-17173.
[14] Otwinowski Z, Minor W. Processing of X-ray diffraction data collected in oscillation mode. Methods Enzymol 1996; 276: 307-326.
[15] Vagin A, Taplyakov A. MOLREP: An automated program for molecular replacement. J Appl Cryst 1997; 30: 1022-1025.
[16] Brunger AT, Adams PD, Clore GM, DeLano WL, Gros P, Grosse-Kunstleve RW, Jiang JS, Kuszewski J, Nilges M, Pannu NS, Read RJ, Rice LM, Simonson T and Warren GL. Crystallography & NMR system: A new software suite for macromolecular structure determination. Acta Crystallogr D Biol Crystallogr 1998; 54: 905-921.
[17] Jones TA, Zou JY, Cowan SW and Kjeldgaard M. Improved methods for building protein models in electron density maps and the location of errors in these models. Acta Crystallogr A 1991; 47: 110-119.
[18] Laskowski R, MacArthur M, Moss D and Thornton J. PROCHECK: a program to check stereo chemical quality of protein structures. J Appl Cryst 1993; 26: 283-291.
[19] Ramachandran GN, Sasisekaran V. Conformation of polypeptides and proteins. Adv Protein Chem 1968; 23: 283-438.
[20] Krissinel E, Henrick K. Inference of macromolecular assemblies from crystalline state. J Mol Biol 2007; 372: 774-797.